# The Effect of the Apparent Baseline on Fringe Amplitude and Period

By
Dana Dawson
Rhonda Tully
July 2004
MST 562

# INTRODUCTION

Since the beginning of time, humans have looked at objects in the sky and wondered about their connection to them. Early astronomers observed the night sky, asked questions and developed the mathematics to answer those questions, which in turn required better methods of observations. Today, as the science of Astronomy expands into new frontiers of discovery, the development of more sophisticated instruments and methods of studying the universe have provided an increasing window of understanding. Through the interesting field of astrophysics called Radio Astronomy, one can detect and understand more about the universe than what the eye can see.

Our main source of energy on earth comes from the sun in the form of particles or waves or a combination of both. While we can detect other forms of energy from distant parts of the universe, electromagnetic radiation in the form of radio waves is the channel of energy used in Radio astronomy. Techniques of using radio waves, such as interferometry, often allow astronomers to probe deeper and further for answers than other techniques developed in recent years.

# PURPOSE

The purpose of this MST Radio Astronomy Project is to use an interferometer to compare the effect that the *apparent* baseline length has on the fringe amplitude and period pattern of radio waves emitted by the sun at different positions in the sky. The radio telescopes will be pointed toward the energy source, in this case the sun, and radio wave data will be collected as the earth's rotation carries the source through the position in the sky that is detectable by the telescopes.

# HYPOTHESIS

It is the hypothesis of this research team that the fringe amplitude will increase when the sun is directly overhead and the radio waves are in phase, and the fringe period will decrease as the amplitude increases.

# RESEARCH BACKGROUND ON RADIO ASTRONOMY

## Electromagnetic Radiation

Energy from the sun and other radio stars or areas of the universe studied in radio astronomy is referred to electromagnetic radiation and is caused from the emission and acceleration of charged particles from a source through electrical and magnetic fields. These particles are characterized by different wavelengths (λ) and classified in ranges in an electromagnetic spectrum (EMS). From these different wavelengths we can also determine the frequency ($\nu$) of radiation emitted. The wavelength is the shortest distance between two corresponding points of a wave where the wave pattern repeats itself, while frequency is determined by the number of waves that pass a given point in a specific time. The unit for frequency (Hz) is named for Heinrich Hertz, an early pioneer in the study of EMS. Frequency and wavelengths are related mathematically; as the wavelength decreases the frequency and energy of the wave increase. All forms of electromagnetic waves travel at the speed of light (c) and this relationship is illustrated in the following equation

$$c=\lambda\nu$$

Waves from the sun that have very long wavelengths and lower frequencies studied in radio astronomy are called radio waves. As the wavelength decreases, the type of radiation defined in the EMS changes from radio waves, a type of radiation including higher frequency microwaves, to infrared, visible light, ultraviolet light, x-rays and high frequency gamma rays. While mechanical waves such as sound waves require a medium in which to travel, electromagnetic radiation travels through a vacuum in space. The following is an image of the EMS showing the range of wavelengths and how they relate to frequency and energy increases.

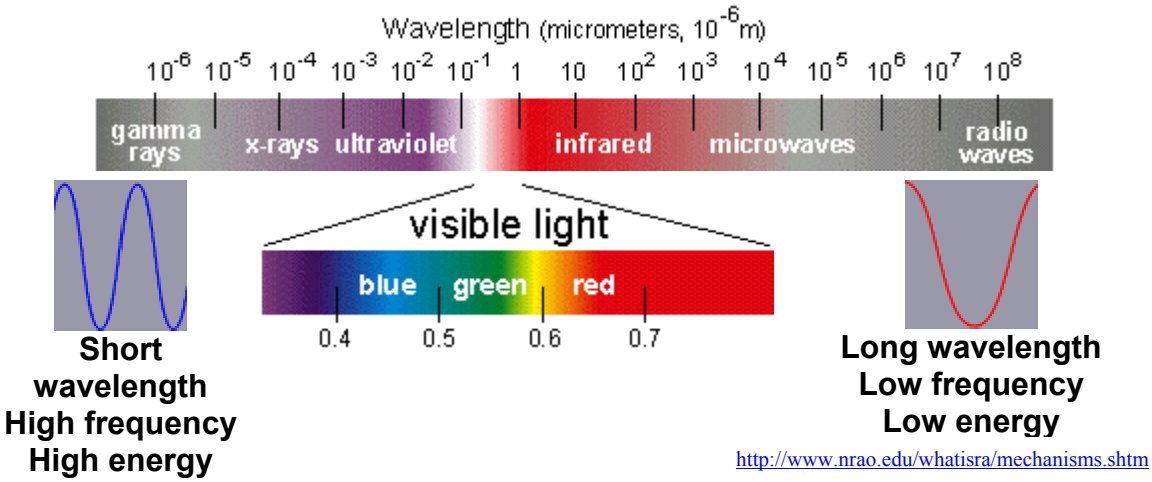


http://www.nrao.edu/whatisra/mechanisms.shtm

The electromagnetic waves in the EMS have special characteristics and properties. A wave is formed when photons, little packets of energy that are always moving, travel with a velocity of 3 x $10^8$ meters/second or the speed of light (c), and move in a perpendicular direction to the oscillation of the electrical and magnetic fields of a radiating source of energy. The atoms that comprise the energy source have electrons that spin about the nucleus in various energy levels or states. When these electrons become excited and absorb or emit energy, they move higher or lower within these energy levels that surround the nucleus of the atom. These moves are accompanied by the absorption or emission of photons. In 1905, Einstein introduced the theory of photons having dual wave-particle characteristics. A few years previously, Maxwell Planck had suggested the idea of a quantum or minimum quantity of energy that can be lost or gained by an atom. He proposed that the energy of these photons is related to the frequency and the wavelength in the following equation:

$$E=h\nu \quad \text{or} \quad \lambda=c/\nu$$

$h=6.63 \times 10^{-27}$ ergs/sec is known as Planck's constant where erg is a unit of energy

The waves in EMS can also be characterized by amplitude, which is the height or displacement of each wave from the rest or equilibrium position. As seen in the following

picture, the high points of each wave motion are called crests and the troughs are the low points. Each crest or each trough is spaced one wavelength distance from the next. The shortest time interval during which a wave motion repeats itself is called the period of the wave. Wave velocity is the product of the frequency and the wavelength.

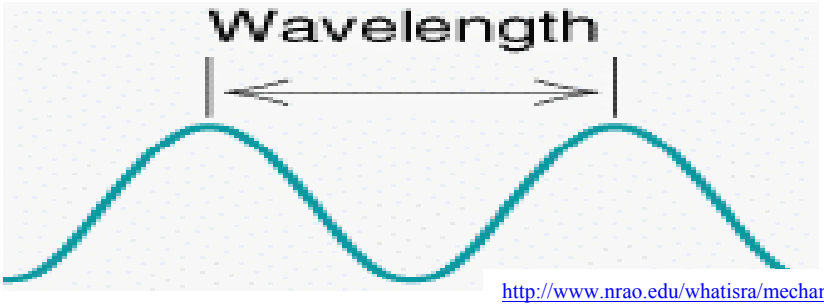


http://www.nrao.edu/whatisra/mechanisms.shtm

In addition, the characteristics of waves allow two or more waves to exist in the same area at the same time. Although each wave has an individual affect in radio emissions they can be superimposed or combined in a way algebraically with different results. This is called wave interference. When the wave displacements are in the same direction, this is called constructive interference. At this point, the waves are in phase with the resulting wave exhibiting a larger amplitude than either individual wave. When two waves overlap, where the displacements are opposite but equal, the result is destructive interference and the waves are now out of phase.

## Optical vs. Radio Telescopes

In years past we were only able to use optical telescopes to see objects in the EMS range of visible light, that range of wavelengths which our eye could detect, but that is only a very small portion of the entire range of electromagnetic radiation that we receive. As mentioned, radio waves have longer wavelengths that are not detected by the human eye, but can be detected by special telescopes that gather information about the phase and amplitude of the radio waves. These radio telescopes have allowed us to broaden our studies of the universe and gather additional information from various astronomical sources.

Similar to how the EMS is defined by regions of increasing wavelength, the radio region of the EMS has its own range of wavelength and frequencies that astronomers use to observe emissions from the sun and other celestial sources of radiation. In the 1930's, radio astronomers and research physicists used various letters of the alphabet to identify the different bands of radio frequency in order to maintain secrecy from the enemy about the radio frequencies they were using in developing radar technology for the military. Common radio band names with their wavelength and frequency counterparts are shown in the illustration below.

| Band | Wavelength | Frequency |
|---|---|---|
| P-band | 90 cm | 327 MHz |
| L-band | 20 cm | 1.4 GHz |
| C-band | 6.0 cm | 5.0 GHz |
| X-band | 3.6 cm | 8.5 GHz |
| U-band | 2.0 cm | 15 GHz |
| K-band | 1.3 cm | 23 GHz |
| Q-band | 7 mm | 45 GHz |

http://www.nrao.edu/whatisra/mechanisms.shtm

Radio telescopes operate in a band of frequency that correlates to the wavelength of incoming radio waves. Since the radio waves have a much greater wavelength than visible light, radio telescopes are designed to collect as much energy as possible and therefore are much larger. Radio telescopes do not have a lens to focus the shorter wavelengths of light, but instead use a parabolic shaped dish or *reflector* to collect and reflect the longer radio waves or power toward a *subreflector* situated close to the prime focus which directs the radiation to a *feed* at the center of the reflector. A receiver behind the feed amplifies the signal and detects the appropriate range of frequency. Next, a computer processes the signal in such a way that it remains in direct proportion to the strength of the radio waves detected. The image produced is a true representation then of the incoming radio waves detected by the reflector.

Another reason radio telescopes are much larger than optical telescopes is related to angular resolution, the angular area of the sky where the radio waves from sources can be detected which is proportional to the wavelength divided by the antenna's diameter. The larger telescopes allow for greater sensitivity and resolution, making them able to detect fainter objects in the sky or distinguish between two objects close together.

In optical telescopes, the wavelengths, which can be detected from the ground are limited to a size of about 4 cm, while radio telescopes allow detection of much larger wavelengths, however the resolving power of radio telescopes becomes less. We compensate in radio astronomy by using telescopes or a combination of telescopes with larger diameters like the Very Large Array near Magdelena, New Mexico, or even larger interferometers like the Very Large Baseline Array, (VLBA) that includes other telescopes with the VLA to make an even larger interferometer.

## Thermal and Non-Thermal Emission

The mechanism for the way that sources emit electromagnetic radiation can be generally classified as either thermal or non-thermal forms of emission. As expected, thermal emission is dependent on the temperature of the emitting source and includes blackbody radiation, free-free emission and spectral line emission. Blackbodies are objects that have a temperature above absolute zero[1] and emit wavelengths in the EMS dependent on their temperature. Cooler objects around 1000 Kelvin emit wavelengths more in the infrared region of the EMS, while hotter objects, like stars, emit mostly visible light. Extremely hot objects like white dwarfs emit high frequency ultraviolet radiation. Free-free emission and spectral line emission are also a result of the transition or movement of electrons from higher energy levels to lower levels, but in a somewhat different fashion than blackbodies. The source of energy in the sun stems from nuclear fusion with hydrogen being converted in a multi-step reaction to helium resulting in temperatures that range from more than 5000 K to over 10,000 K.

Non-thermal emissions are a result of charged particles moving in a magnetic field, which also causes the electron to accelerate and change direction as they spiral around

the field. The frequency of the emission is related to the velocity of the electrons traveling near the speed of light. Non-thermal forms of emission include synchrotron emission from supernova remnants, quasars, or active galactic nuclei (AGN), and gyro-synchrotron emission emitted by pulsars, which are a result of the death of massive stars as they run out of fuel and their cores begin to collapse. Masers (microwave amplification by stimulated emission of radiation) are a third form of non-thermal emission and are intriguing objects that amplify faint emission from distant sources at specific frequencies. Masers are molecules, acting as a group like energized electrons, that become energized and move to lower energy levels emitting a photon, which in turn produces a domino effect on nearby molecules causing them to also change energy levels. In order for these masers to return to their original energy state, they rely on outside energy sources like a star to provide the energy to enable their move. Groups of molecules identified to act like masers include the hydroxyl radical (OH), water, methanol, formaldehyde, silicon oxide and ammonia.

## Sensitivity and Resolution

As mentioned earlier, in order to observe objects that are often very small and/or that are very faint, astronomers need to maximize the light gathering power and resolving power of the telescope. If one increases the collecting area of a dish, one can increase the amount of radiation that is focused onto the receiver, thus enhancing the sensitivity of the telescope. To make accurate measurements one must be able to distinguish objects. The ability to distinguish objects is called the telescope's resolution and this also depends on the linear size of the collector. This relationship is given by

$$\Theta = \frac{\lambda}{D}$$, where θ=angle between sources and D=diameter of the dish

To achieve an increase in the sensitivity and resolution of a telescope one can build bigger dishes – up to a limit. Due to structural limits, telescopes can only be built up to a few hundred meters or so. The larger the size of a telescope presents many challenges, especially if one wants to move or redirect a telescope to observe different parts of the

sky. The largest radio telescope is the Arecibo telescope in Puerto Rico, which is 308 m in diameter.

## Interferometry

Obviously the angular resolution of a single telescope, even the largest that could possibly be built, is insufficient to meet the needs of astronomy. The solution is achieved by using the principle of interferometry. A simple interferometer involves the combining of signals from two telescopes. The distance between the telescopes, combined in this fashion, effectively becomes the diameter of the collection instrument.

Interferometry is derived from the word interference. Interference is a phenomenon that occurs when multiple waves come together at the same time and at the same place. One can think of interference as the adding of waves. As shown in the following figure, when waves are in phase, meaning that the crests of the waves coincide, the sum of the waves is a similar wave but with an increase in amplitude. This is called constructive interference. If the crests of the waves are exactly out of phase, meaning the crest of one wave coincides with the trough of the other wave, the net displacement is exactly zero when the waves are added. This is called destructive interference.

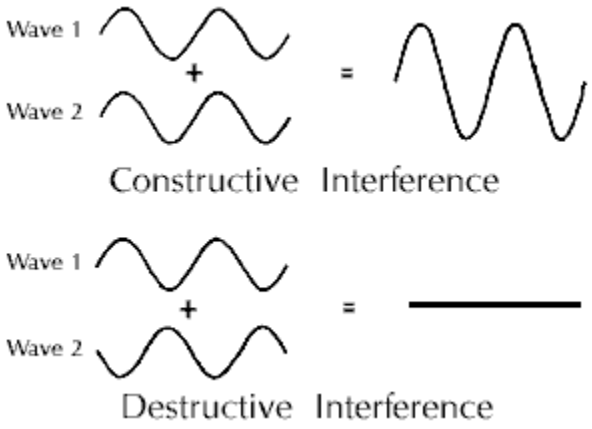


http://www.space.com/scienceastronomy/astronomy/interferometry_101.html

The amount of interference depends on how out of phase the waves are with respect to each other and their amplitudes.

When radio waves arrive from a source, the waves arrive alternately in phase and out of phase due to the rotation of the Earth. The addition of these waves produces interference fringes. Maxima in the fringes result from interference for which the difference in the path length from the source to the point at which the waves are combined is an integral number of wavelengths, meaning the waves are in phase. Shown are fringes, as obtained by an optical telescope. Fringes obtained from radio telescopes demonstrate a similar pattern.

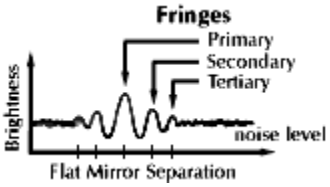


http://www.space.com/scienceastronomy/astronomy/interferometry_101.html

As a measure of relative amplitude of the fringes, one can use the following equation:

$$\text{Relative Fringe}_{\text{amplitude}} = \frac{Power_{\max} - Power_{\min}}{Power_{\max} + Power_{\min}}$$

Visibility fringe amplitude is given as follows:

$$\text{Visibility Fringe Amplitude} = \frac{\sin(\frac{\pi b \alpha}{\lambda})}{\frac{\pi b \alpha}{\lambda}},$$

where b=apparent baseline

λ=observing wavelength

ά=source size.

The following can be used to calculate the period of the fringe:

$$\text{Fringe Period} = \frac{\lambda}{b\cos\zeta\omega_E \cos H_o}$$

Where t = time

b=separation of the dishes

ς=angle of declination of the Sun

$\omega_E$=how fast the Earth turns

$H_0$=hour angle

If the source has finite size, the distance traveled by the radio waves to the elements of the interferometer will vary. As shown in the figure below, the wavefront from the source in direction θ reaches the right-hand element before it reaches the left-hand element. Also shown is the baseline between the elements and the projected or apparent baseline between the elements. Notice that the apparent baseline length is calculated based on θ, which is measured from north to the source. The apparent baseline will be different based on orientation of the source to the earth.

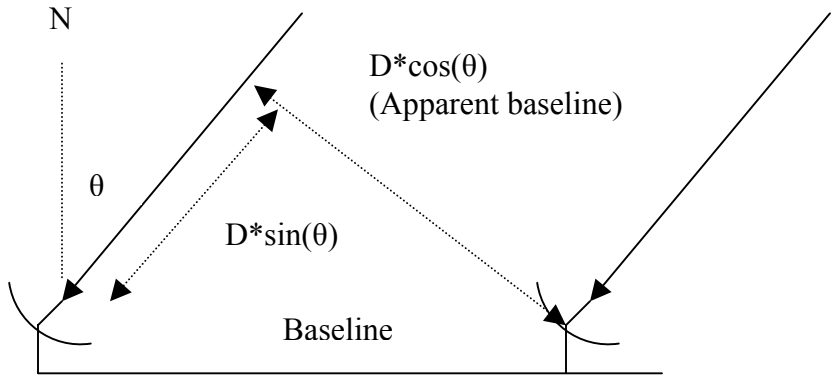


D (Distance between elements)

# Procedure

## Equipment/Materials

- Interferometry consisting of 2 SRT telescopes
    - Specification of SRT telescopes:
        - Aperture: 2.1 meters
        - LO Frequency Range: 1370-1800 MHz
        - LO Tuning Step: 40 kHz
        - Preamp Frequency Range: 1400-1440 MHz
        - System Temperature: 150 K
        - Point Accuracy: 1 Degree
        - Travel Limits (degrees) ~91-269 Azimuth/~0-179 Elevation
- Attenuator, connected in-line with the coaxial cable connected to the SRTs.

## Procedure for Setting Up Interferometer:

1. Connect both SRTs to the computers.
2. Set the attenuator to 0 Db.
3. Turn computers on.
4. Open and set-up the Spectra Cyber Program.
    a. Set the mode to "continuum." (Settings – Mode – Continuum)
    b. Set the integral to 10 sec. (Settings – Integral – Continuous – 10)
    c. Give the data file a name. (Options – online – enter filename)
    d. Set the time step to 3 seconds. (Options – online – enter time step)
    e. Turn autosave on. (Scan – autosave – on)
5. Open and set-up the SRT Program
    a. In command prompt, go to the SRT folder (cd c:\srt)
    b. Type: java srt 0.
    c. The motors will turn on and will stow the interferometer.
    d. After the telescopes are stowed, click on the sun to move the interferometer to point to the sun.

6. Track the sun for awhile to make sure the system is working – meaning power is detected and that it is not saturated. Adjust the attenuator by increments of 1 until the power is being detected and that it is not saturated.
7. Stop collecting data. (Scan – stop)
8. Record the attenuator setting.

## Procedure for collecting data for Drift Scans

Once the system is calibrated (Step 1-8 above) Drift Scan data can be collected. For the purposes of this experiment fringes were to be collected at local noon (1:00 pm MST) when the source crossed the meridian, 2 hours before the crossing (11:00 am MST), and 2 hours after the crossing (3:00 pm MST). The actual times of the experiment were dependent on when the sun was actually crossing the meridian, which turned out to be about 1:09 pm MST.

9. On Spectra Cyber, name a new file for the observation. (Options – online – enter filename)
10. On SRT, Click on Drift to point the interferometer to 5 degrees ahead of the sun.
11. On Spectra Cyber start collecting data. (Scan – Start)
12. Print the SRT setting to capture initial conditions for the experiment. (Click on the PrtScrn key on the keyboard.) Open a Word document and click on Edit – Paste to paste a picture of the screen into the document. Save the word document.
13. After sufficient data is collected, stop the data collection. (Scan – Stop)

Repeat steps 9-12 for each observation.

When all observations are complete:

1. Transfer data files to appropriate location for manipulation. The default location of the data files is C:/documents and settings/user1/desktop/Spectra Cyber/Data
2. Transfer the Word document that contains the print screens to an appropriate location.
3. Stow the telescopes by typing in the appropriate azel settings.
4. Turn the computers off.

# Data

## Observations

Using the Spectra Cyber software for data acquisition, several sets of data were collected. This included:

1. A drift scan of the Sun at 16 40 UTC (10:40 am MST)
2. A drift scan of the Sun at 17 07 UTC (11:07 am MST)
3. A tracking scan of the Sun at 18 06 UTC (12:06 pm MST)
4. A drift scan of the Sun at 19 09 UTC (1:09 pm MST)
5. A drift scan of the Sun at 21 16 08 UTC (3:16 pm MST)
6. A drift scan of the Sun at 21 31 UTC (3:31 pm MST)
7. A tracking scan of the Sun at 21 49 UTC (3:49 pm MST)

## Drift Scan versus Tracking Scan

For a drift scan, the antenna is pointed to 5 degrees ahead of the position of the Sun and collects data as the Sun moves through this position. In this configuration, interference patterns can be observed thus providing fringe information.

The interferometer follows the object being observed throughout the session, collecting point source emission data.

## Data File Specifications

Each data file contained the following information:

The first line includes:

| | | | | | | | | | | | |
|---|---|---|---|---|---|---|---|---|---|---|---|
| C | Month | Date | Year | Hr (UTC) | Min (UTC) | Sec (UTC) | Time step | 0 | 360 | 0 | 5 |

The rest of the file includes power in volts, one number per line, for 360 time steps.

The following graphs were created from the data collected during the observations.

## Data from Individual Observations

Observation 1
A drift scan of the Sun at 16 40 UTC (10:40 am MST)

In test runs to determine power levels of the sun, it was determined that the inline attenuator needed to be set > 0 dB. The attenuator was set to 1 dB at the start of this observation. At about 9 minutes into the run, the power level was saturated. The attenuator was then set to a level of 2 dB. Notice the sharp decrease in the power level at this time.

Atmospheric conditions at this time were clear and sunny.

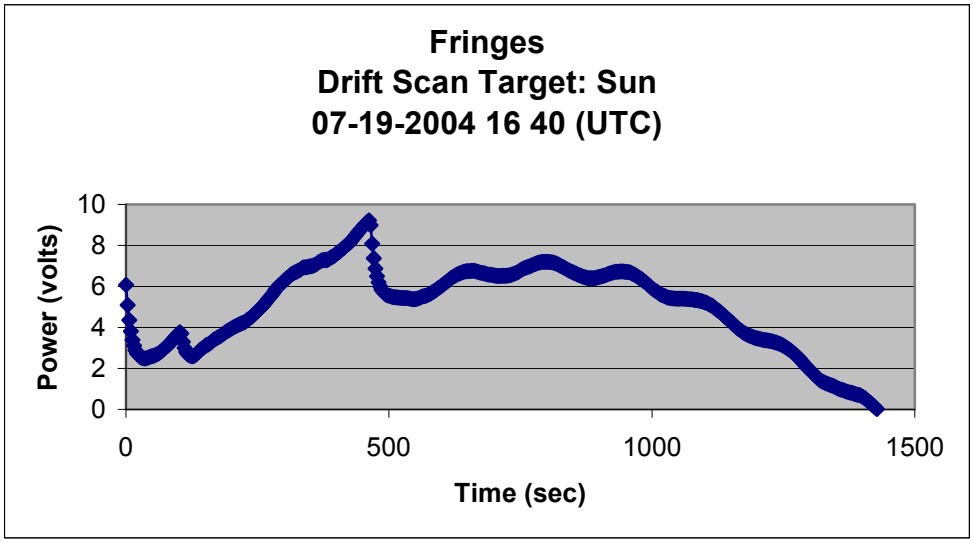


The following figure represents the power levels for t > 550 sec of the first observation after the attenuator was set to 2dB.

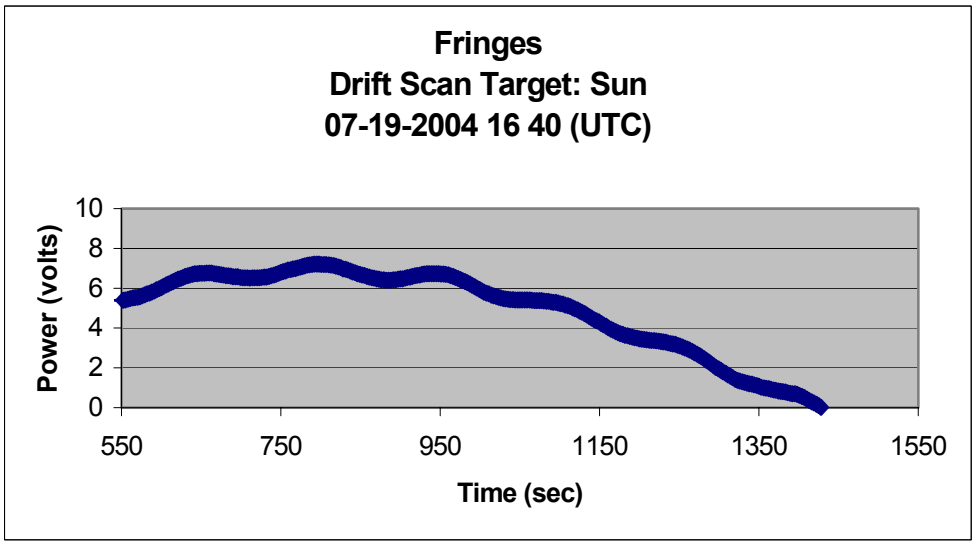


Antenna coordinates:
cmd 103.9 56 deg
azel 103.8 56 deg
Total offset 0.0 0.0
Pointing corr 0.0
Axis corr 0.0
Galactic l=200 b=22
radec 7.8 hrs 20.7 deg

Time UTdate Jul 19
UT 2004:201:16:40

Source
Sun

azel 104.9 57.0 deg
Center frequency:
1420.000 MHz
spacing: 40.00 kHz
number bins: 1
integ. Period: 0.10 sec
tsys: not yet
calibrated

VLSR: 11.0 km/s
Vcenter: 74.6 km/s

The above indicates the antenna and sun coordinates. Also shown is the right ascension and declination of the source (radec), the frequency at which data was collected, the azel of both the interferometer and source.

Observation 2

A drift scan of the Sun at 17 07 UTC (11:07 am MST)

Atmospheric conditions at this time were clear and sunny.

This data set lacks definition.

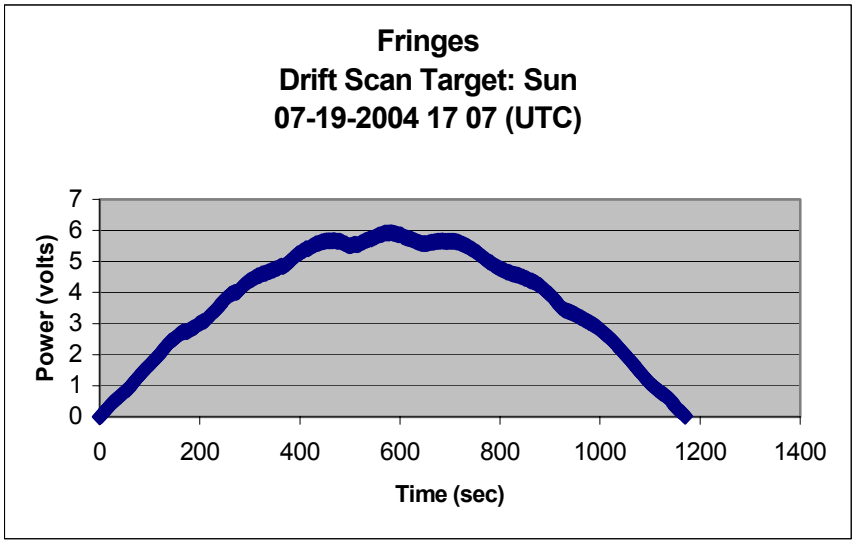


Antenna coordinates:
cmd 110.2 61.2 deg
azel 110.2 61.2 deg
total offsets: 0.0 0.0
pointing corr 0.0 0.0
axis corr 0.0 0.0
Galactic l = 200 b = 21
radec 7.8 hrs 20.7 deg

Time: UTdate Jul 19
UT 2004:201:17:07:35
LST 5.9 hrs

Source:
Sun

azel 107.4 59.1 deg
Center frequency:
1420.000 MHz
spacing: 40.00 kHz
number bins: 1
integ. period: 0.10 sec
tsys: not yet calibrated

VLSR 9.7 km/s
Vcenter 76.0 km/s

Observation 3
A tracking scan of the Sun at 18 06 UTC (12:06 MST)

While waiting for the next time to gather drift scan information, we set the interferometers on autotrack to continually collect data on the Sun. This information will be used as background information in comparing and analyzing the drift scans as well to determine if the interferometer was working properly. The fringe for this tracking looked quite good and the system appears to be working properly.

Atmospheric conditions during this observation were clear and sunny.

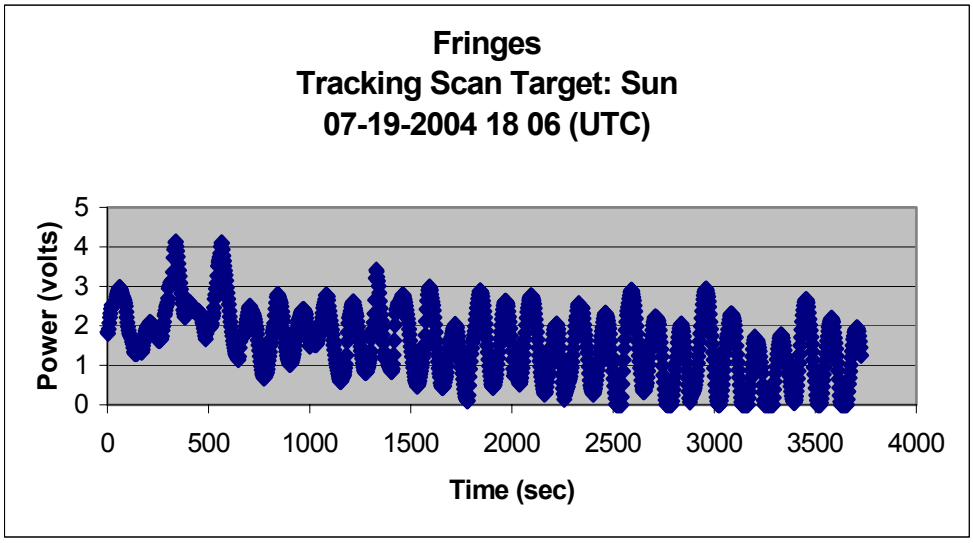


Antenna coordinates:
cmd 130.3 70.7 deg
azel 130.3 70.7 deg
Total offset 0.0
Pointing corr 0.0
Axis corr 0.0
Galactic l=200 b=
radec 8.0 hrs 20.7 deg

Time UTdate Jul 19
UT 2004:201:18:06

Source
Sun

azel 130.5 70.9 deg
Center frequency:
1420.000 MHz
spacing: 40.00 kHz
number bins: 1
integ. Period: 0.10 sec
tsys: not yet
calibrated

VLSR: km/s
Vcenter: km/s

Observation 4
A drift scan of the Sun at 19 09 UTC (1:09 MST)

Ureka! This is lovely! The great fringe pattern noticed during the previous tracking observation continues with this drift scan.

The timing of this observation coincided with the sun's azel at or near 180° 76.6 at local noon (1:09 MST), when the apparent baseline is equivalent to the actual baseline.

Atmospheric conditions were clear and sunny.

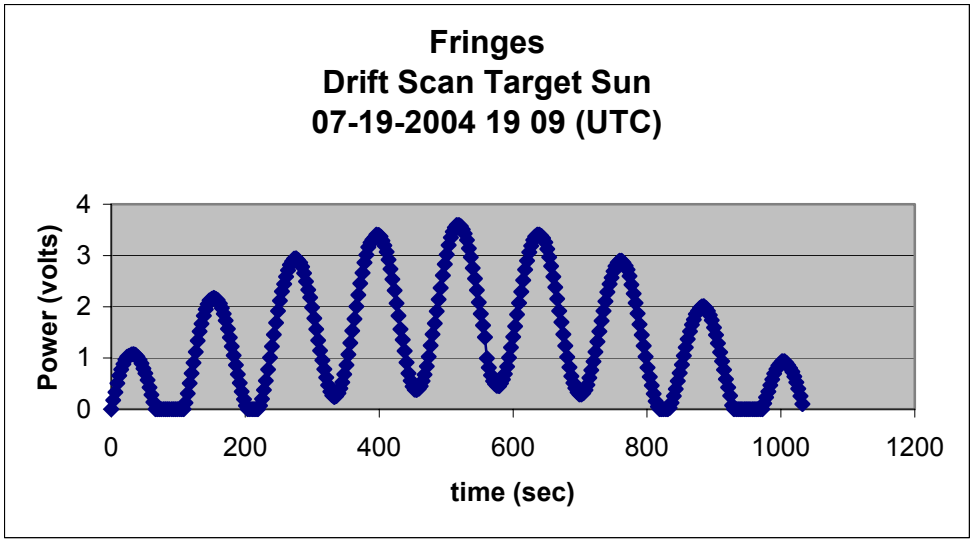


Antenna coordinates:
cmd 187.1 76.5 deg
azel 186.8 76.6 deg
total offsets: 0.0 0.0
pointing corr 0.0 0.0
axis corr 0.0 0.0
Galactic l = 200 b = 21
radec 7.8 hrs 20.7 deg

Time: UTdate Jul 19
UT 2004:201:19:10:20
LST 7.9 hrs

Source:
Sun

azel 176.3 76.6 deg
Center frequency:
1420.000 MHz
spacing: 40.00 kHz
number bins: 1
integ. period: 0.10 sec
tsys: not yet calibrated

VLSR 9.7 km/s
Vcenter 76.0 km/s

Observation 5
A drift scan of the Sun at 21 16 08 UTC (3:16 pm MST)

This observation was terminated prematurely, because of lack of definition in the data and another was started immediately in order to have enough time to collect data before the window of time for observation expired.

This fringe is noticeably different but comparable to the fringe of the next observation. Both of these observations coincided with escalating weather conditions.

Atmospheric conditions began to degrade during this observation. Clouds moved in, a breeze was noticed.

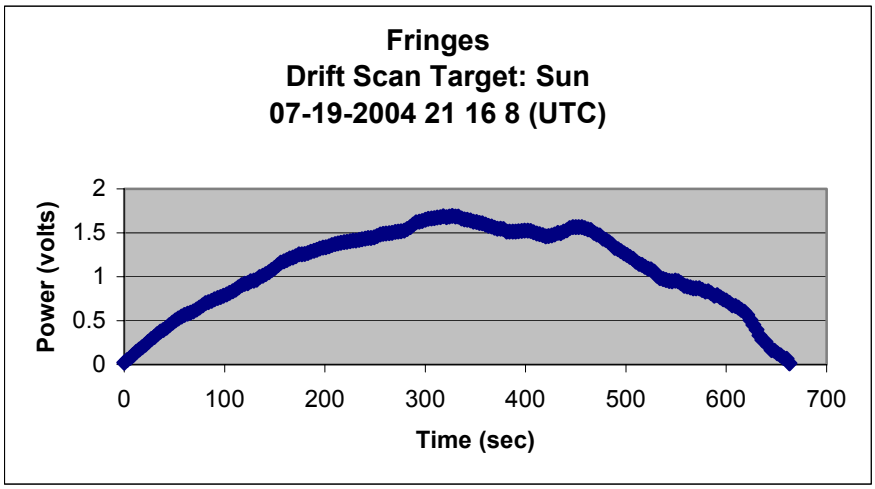


Antenna coordinates:
cmd 253.7 58.1 deg
azel 253.6 58.2 deg
total offsets: 0.0 0.0
pointing corr 0.0 0.0
axis corr 0.0 0.0
Galactic l = 200 b = 21
radec 7.8 hrs 20.6 deg

Time: UTdate Jul 19
UT 2004:201:21:14:19
LST 10.0 hrs

Source:
Sun

azel 251.0 60.3 deg
Center frequency:
1420.000 MHz
spacing: 40.00 kHz
number bins: 1
integ. period: 0.10 sec
tsys: not yet calibrated

VLSR 9.7 km/s
Vcenter 76.0 km/s

Observation 6
A drift scan of the Sun at 21 31 UTC (3:31 MST)

This drift scan was started soon after the previous observation was terminated in hopes that a better-defined curve would be acquired.

Again the fringe was different from the fringe taken at 1:09 MST. We are not sure what extraneous interference is causing the difference, if any.

Atmospheric conditions continued to deteriorate. Lightening/thunder and intermittent rain was observed.

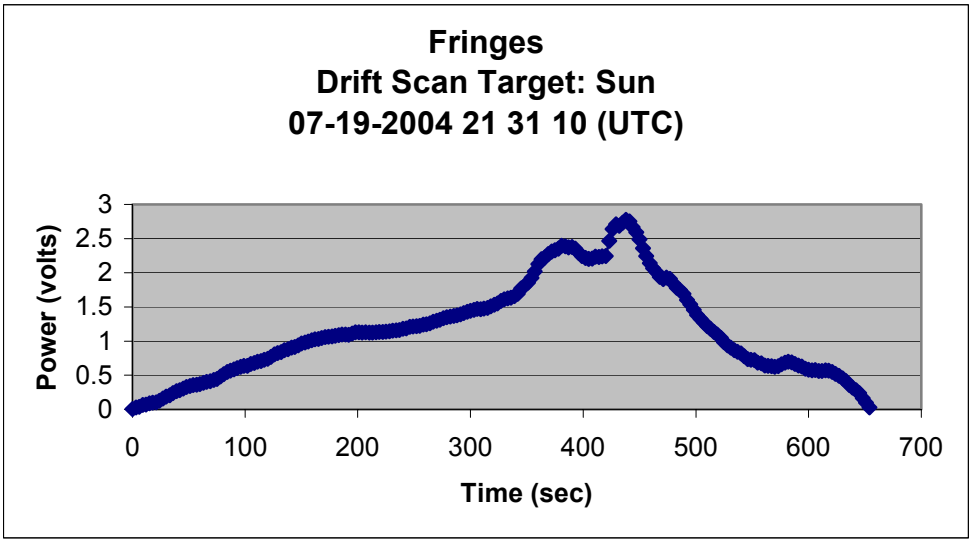


Antenna coordinates:
cmd 257.4 54.8 deg
azel 257.4 54.8 deg
Total offset 0.0 0.0
Pointing corr 0.0 0.0
Axis corr 0.0 0.0
Galactic 1=200 b=
radec 8.0 hrs 20.6 deg

Time UTdate Jul 19
UT 2004:201:21:31

Source
Sun

azel 255.4 56.6 deg
Center frequency:
1420.000 MHz
spacing: 40.00 kHz
number bins: 1
integ. Period: 0.10 sec
tsys: not yet
calibrated

VLSR: km/s
Vcenter: km/s

Observation 7

A tracking scan of the Sun at 21 49 UTC (3:49 MST)

Due to the unusual patterns detected in observations 5 and 6, the interferometer was set to track the sun in order to determine if the system was functioning properly.

Allowed to continue on autotrack, the fringe became somewhat more symmetric as time elapsed.

Atmospheric conditions required the shut down of the system due to lightening and strong winds.

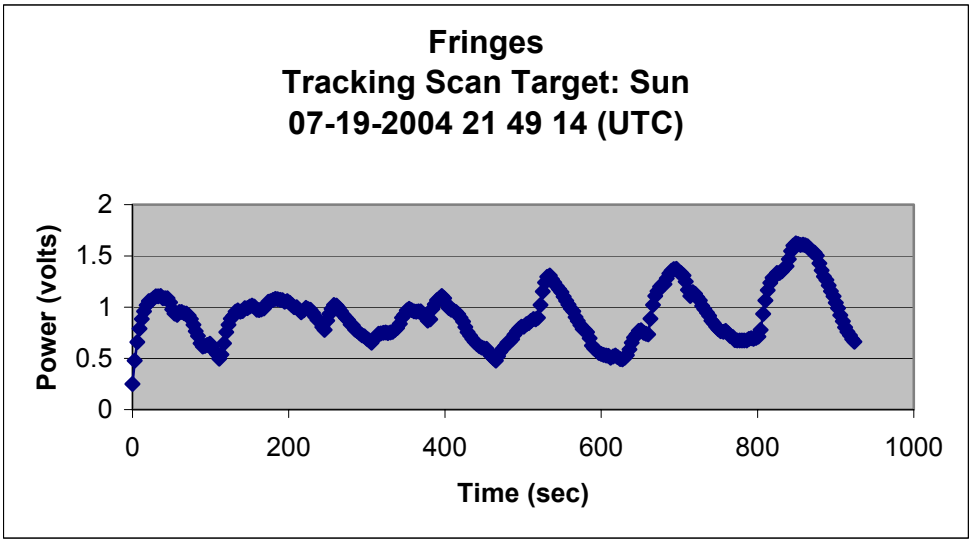


Antenna coordinates:
cmd 258.8 53.2 deg
azel 258.8 53.2 deg
total offsets: 0.0 0.0
pointing corr 0.0 0.0
axis corr 0.0 0.0
Galactic l = 201 b = 24
radec 8.0 hrs 20.6 deg

Time: UTdate Jul 19
UT 2004:201:21:49:32
LST 10.6 hrs

Source:
Sun

azel 258.8 53.2 deg
Center frequency:
1420.000 MHz
spacing: 40.00 kHz
number bins: 1
integ. period: 0.10 sec
tsys: not yet calibrated

VLSR 10.6 km/s
Vcenter 75.1 km/s

# Results

The purpose of this project is to determine the effects in fringe amplitude and period due to a change in the projected baseline length.

Apparent Baseline

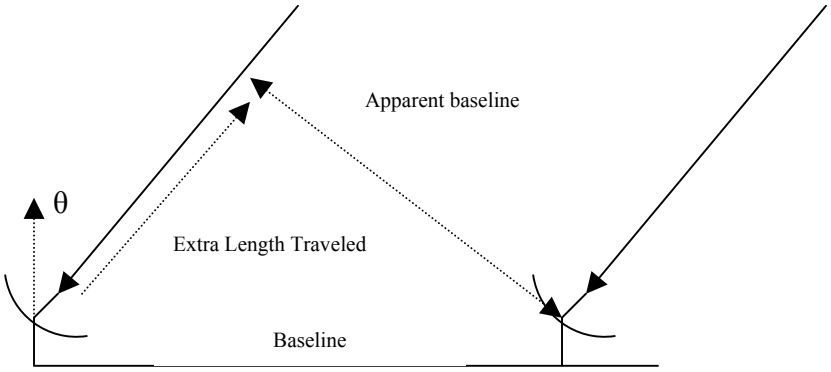


D (distance between elements)= 24 m

Extra length traveled = cos(dec of the sun)*sin(hour angle of the sun)*apparent baseline
Apparent baseline = $\text{baseline}^2$-$\text{extra length traveled}^2$

As shown below, the apparent baseline did vary throughout the experiment. The maximum apparent baseline approached the actual baseline at noon standard time or 1:09 pm daylight savings time. Also shown is the extra length traveled by the radio waves to reach the second element of the interferometer.

| Drift Observation Number | Time (MST) | Length of Apparent Baseline (m) | Extra Length Traveled (m) |
|---|---|---|---|
| 1 | 10:40 am | 19.47 | 14.04 |
| 2 | 11:07 am | 21.18 | 11.29 |
| 3 | 1:09 pm | 23.99 | 0.59 |
| 4 | 3:16 pm | 21.16 | 11.31 |
| 5 | 3:31 pm | 19.16 | 14.46 |

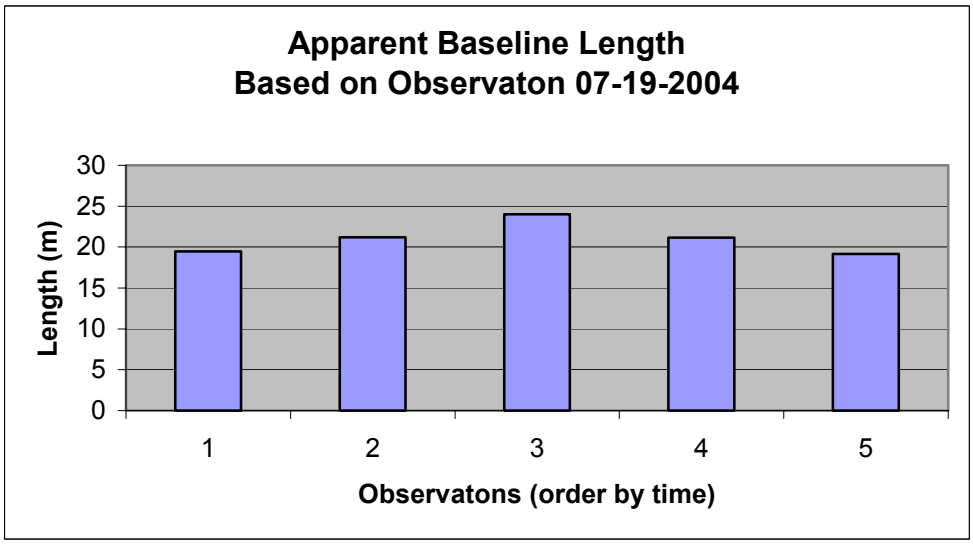


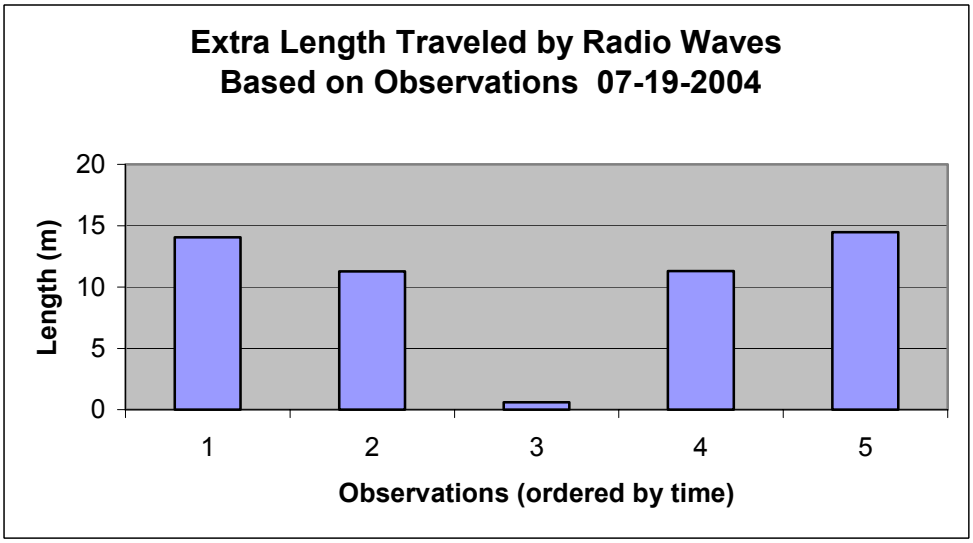


Fringe Amplitude

The fringe amplitude was measured from the primary fringe as follows:

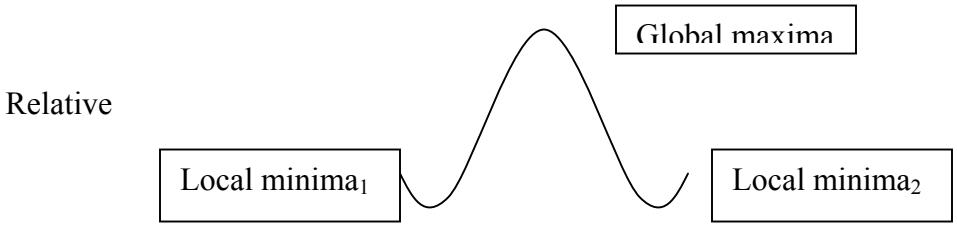

$$\text{Fringe}_{\text{amplitude}} = \frac{Power_{\max} - Power_{\min}}{Power_{\max} + Power_{\min}}$$

The average fringe amplitude is calculated by adding the fringe amplitude as measured to the left of the primary fringe and the fringe amplitude as measure to the right of the primary fringe and then dividing by two.

| Drift Observation Number | Time (MST) | Average Fringe Amplitude (volts) |
|---|---|---|
| 1 | 10:40 am | 0.054962 |
| 2 | 11:07 am | 0.033448 |
| 3 | 1:09 pm | 0.794073 |
| 4 | 3:16 pm | 0.055598 |
| 5 | 3:31 pm | 0.150002 |

The primary fringe amplitude varied with the apparent baseline length. The maximum fringe amplitude occurred when the apparent baseline was the longest.

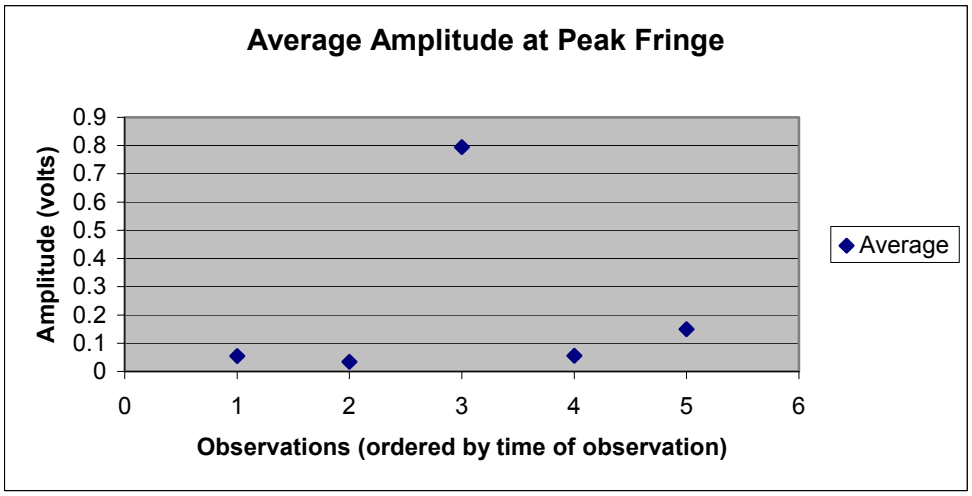

The observed amplitudes follow the same trend as does the theoretical for the first two and last two observations, but is significantly different for the third observation.

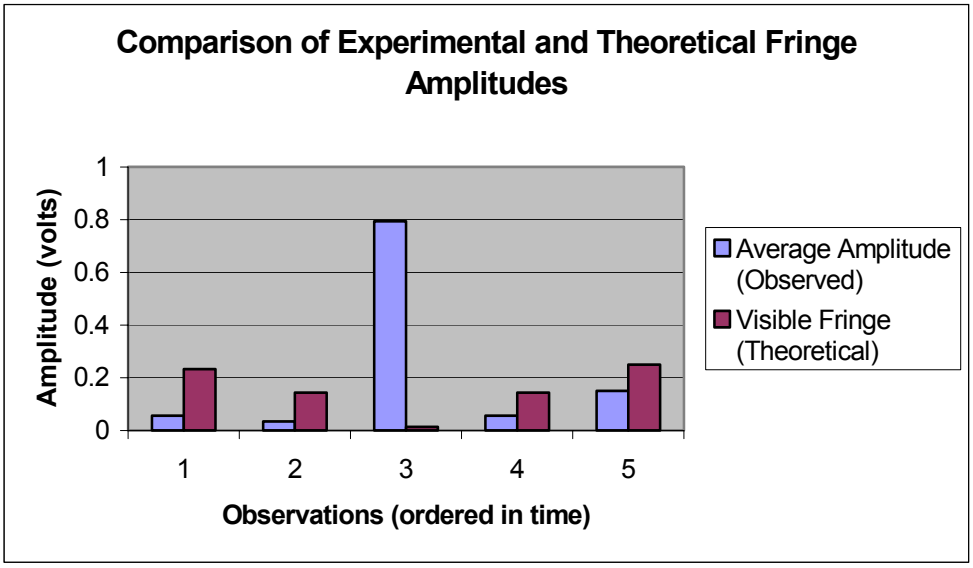


Shown below is a comparison of the ratio of $amplitude_t/amplitude_{t+1}$ for both the observed and theoretical amplitudes. This was done in order to compare relative sizes of the amplitudes. This reinforces that the trends are comparable for the first two observations and the last two observations and significantly different for the third observation.

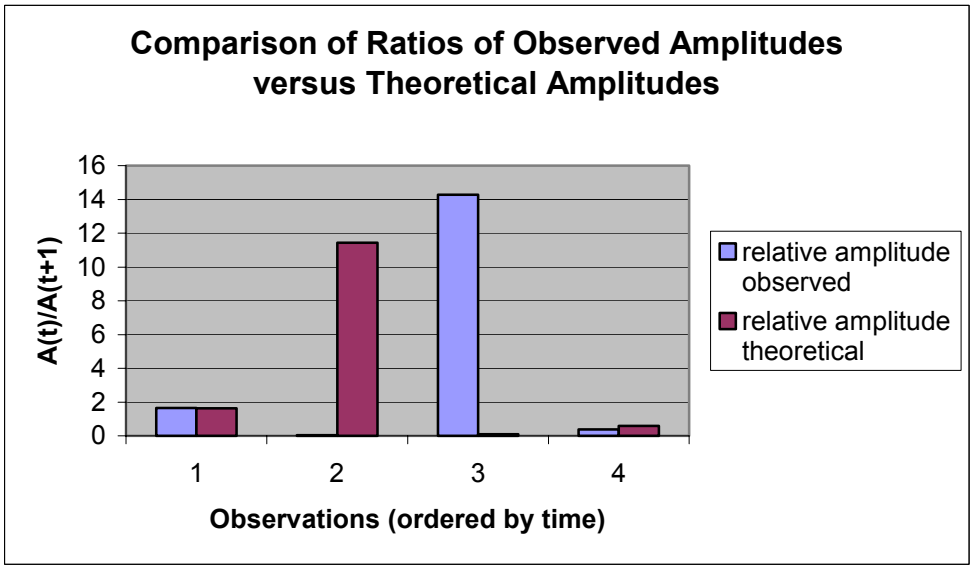

Fringe Period

The average fringe period was calculated as shown.

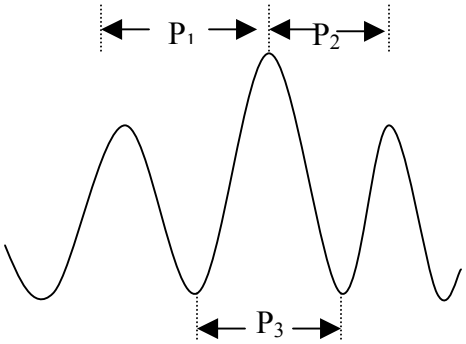


The period was calculated by determining the time between adjacent maxima or adjacent minima.

| Drift Observation Number | Time (MST) | Average Period Length (sec) |
|---|---|---|
| 1 | 10:40 am | 152 |
| 2 | 11:07 am | 131 |
| 3 | 1:09 pm | 121 |
| 4 | 3:16 pm | 72 |
| 5 | 3:31 pm | 53 |

The average period of the fringe decreased during the observation day. This trend does not correlate with the change in the apparent baseline of the interferometry.

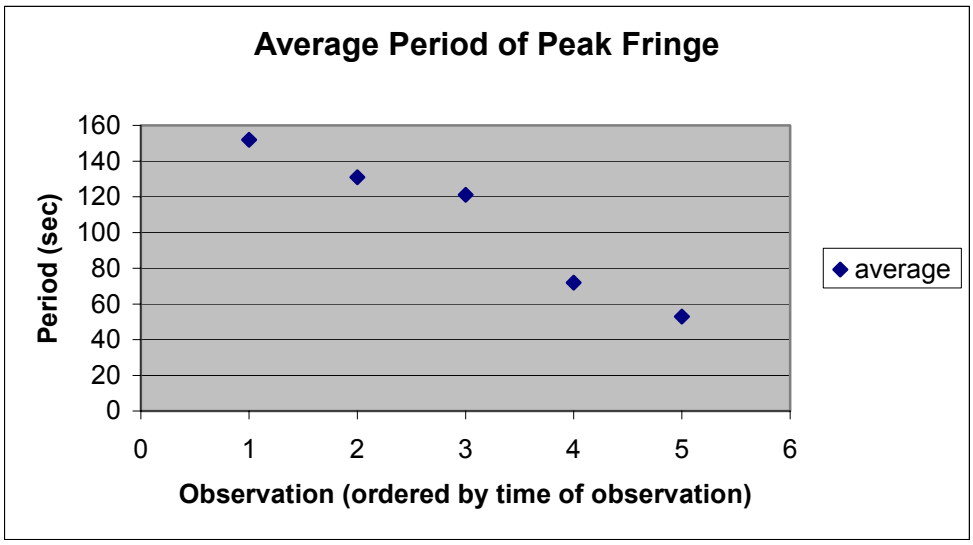


The experimentally observed fringe periods agree with the theoretical values somewhat for the first three observations but is significantly different for the last two observations.

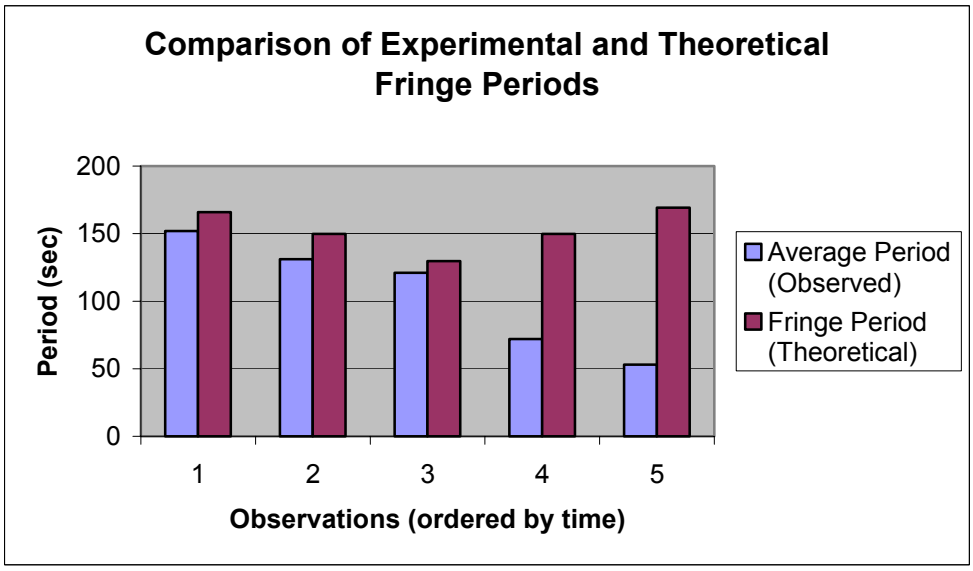

# CONCLUSION

The amplitude of the fringe pattern collected with the interferometer did increase during the observation where the apparent baseline was close to the actual baseline, and the fringe period did decrease as the amplitude increased as expected. Deviations from the expected as presented in the results may be resolved through further observations and research into possible interference sources that might have caused the late afternoon fringe patterns to vary from those collected at local noon.

# EXTENSIONS

The project may be extended through further observations of the sun at similar times, observations of other radio sources and their fringe patterns, plus a review of the tracking data to make similar comparisons of fringe and amplitude variations in relation to the apparent baseline length.

## Works Cited


Feynman, Richard P. Six Easy Pieces . Reading: Addison-Wesley Company, 1995. 1-138.

Goss, W W. Ruby Payne-Scott. National Radio Astronomy Observatory. MST Radio Astronomy Course. NRAO, Socorro, NM. 12 July 2004.

Moran, James M., George W. Swenson,Jr., and A. Richard Thompson. Interferometry and Synthesis in Radio Astronomy. New York: John Wiley and Sons, Inc., 2001.

NRAO:Why Do Astronomy. 5 Mar. 2004. National Radio Astronomy Observatory. 6 July 2004 <http://www.nrao.edu/whatisra/valueofastro.shtml>.

NRAO Glossary. 29 July 2003. National Radio Astronomy Observatory. 07 July 2004 <http://www.nrao.edu/imagegallery/glossary.shtml>.

Prehistory of Radio Astronomy. 26 June 2003. National Radio Astronomy Observatory. 06 July 2004 <http://www.nrao.edu/whatisra/hist_prehist.shtml>.

Radio Astronomy and Interference. 03 Sept. 2003. National Radio Astronomy Observatory. 07 July 2004 <http://www.nrao.edu/whatisra/rfi.shtml>.

Radio Astronomy FAQ. 28 May 2004. National Radio Astronomy Observatory. 6 July 2004 <http://www.nrao.edu/whatisra/radiotel.shtml>.

Radio Emission. 15 July 2003. National Radio Astronomy Observatory. 06 July 2004 <http://www.nrao.edu/whatisra/mechanisms.shtml>.

The Physics Classroom. 2004. The Physics Classroom and MacIntosh Engineering and Education, Inc. 06 July 2004 <http://physicsclassroom.com.com/Class/light/lighttoc.html>.

The World Treasury of Physics, Astronomy, and Mathematics. Boston:Little, Brown and Company, 1991.

Undergraduate Research Educational Initiative Radio Astronomhy Tutorial. 23 Aug. 2000. Undergraduate Research Educational Initiative. 6 July 2004 <http://web.haystack.mit.edu/urei/tut2.html>.

Westphal, David. The Adding Radio Interferometer. National Radio Astronomy Observatory. NRAO, Socorro, NM.

What is Radio Astronomy? 11 Mar. 2003. National Radio Astronomy Observatory. 7 July 2004 <http://www.nrao.edu/whatisra/radiotel.shtml>.